Journal of Materials Science and Chemical Engineering, 2026, 14(2), 90-107
https://www.scirp.org/journal/msce
ISSN Online: 2327-6053
ISSN Print: 2327-6045

Characterization of Local Clay from Burkina Faso for the Removal of Lead from Groundwater

Arzouma Christophe Guissou[1], Dimanche Regie Ouedraogo[2,3], Brahima Sorgho[1*], Yacouba Soutra[4]

[1]Equipe Physico-Chimie et de Technologie des Matériaux, Laboratoire de Chimie Moléculaire et des Matériaux (LCMM), Unité de Formation et de Recherche en Sciences Exactes et Appliquées (UFR-SEA), Université Joseph KI-ZERBO, Ouagadougou, Burkina Faso
[2]Équipe Chimie Physique et Électrochimie, Laboratoire de Chimie Moléculaire et des Matériaux (LCMM), Unité de Formation et de Recherche en Sciences Exactes et Appliquées (UFR-SEA), Université Joseph KI-ZERBO, Ouagadougou, Burkina Faso
[3]Kaya University Center, Joseph KI-ZERBO University, Ouagadougou, Burkina Faso
[4]Direction de la Recherche Géologique et Minière (DRGM), Bureau des Mines et de la Géologie du Burkina (BUMIGEB), Ouagadougou, Burkina Faso
Email: *sorghobrahima3@mail.com

How to cite this paper: Guissou, A.C., Ouedraogo, D.R., Sorgho, B. and Soutra, Y. (2026) Characterization of Local Clay from Burkina Faso for the Removal of Lead from Groundwater. *Journal of Materials Science and Chemical Engineering*, **14**, 90-107.
https://doi.org/10.4236/msce.2026.142006

Received: December 29, 2025
Accepted: February 24, 2026
Published: February 27, 2026

Abstract

The contamination of water resources by trace metals (TMs), particularly lead (Pb^{2+}), is a significant public health and environmental concern, especially in areas where access to modern treatment technologies is limited. The adsorbent material used is KOM clay, collected from Kombissiri, near Ouagadougou, in Burkina Faso, and characterized using various physicochemical techniques. Characterization enabled the quantification of the minerals present in KOM: quartz (27%), montmorillonite (25%), illite (21%), kaolinite (18%), and goethite (6%). This characterization highlighted the adsorbent properties of montmorillonite clay, which endow it with an interesting adsorption capacity for removing lead from groundwater. Adsorption tests carried out in synthetic batch solutions showed that the adsorption capacity of lead (Pb^{2+}) is influenced by various parameters, namely kinetics, dose effect, and initial concentration effect. The kinetic study showed that contact time is reached after 3 hours. The data were consistent with the pseudo-second-order model. The results obtained by dose effect show that clay could remove up to 98.03%, or 4.9 mg/g, for an optimal adsorbent dose of 10 g/L. The isotherm models obtained from the data on the effect of the initial concentration on the adsorption of lead Pb^{2+} confirmed that the adsorption of lead Pb^{2+} is monolayer adsorption. This result reflects a strong affinity between lead and the active sites of montmorillonite and confirms the value of this natural material as an economical and sustainable solution for treating water polluted by trace metals.

Keywords

Water, Adsorption, Montmorillonite Clay, Lead, Burkina Faso

1. Introduction

Clays are natural raw materials widely used by local populations for various purposes. However, clay is not a standardized material; its composition varies depending on the geographical location, and its formation is part of the geological processes of the Earth's crust, which is mainly composed of silicate rocks [1] [2]. Recent studies have reported the physicochemical characterization of several clays from Burkina Faso, as well as their potential applications in housing construction, road and track stabilization, and the treatment of water contaminated with inorganic pollutants [1]-[3]. In construction and civil engineering applications, clays are also recognized for their adsorptive properties, particularly in the removal of heavy metals through specific adsorption mechanisms [4]. Several studies have demonstrated their effectiveness in trapping pollutants from contaminated water due to these adsorption properties [3] [4].

Despite these advantages, the use of montmorillonite-rich clays for decontaminating water polluted with inorganic contaminants remains limited in Burkina Faso. Most existing studies have focused on kaolinite clays for lead removal, with little attention paid to montmorillonite clays, despite their well-known high adsorption capacity for Pb^{2+} ions in aqueous solutions [5] [6]. The application of montmorillonite-containing clays for lead-contaminated water treatment requires a thorough understanding of their chemical and mineralogical characteristics. However, to the best of our knowledge, there is a lack of scientific data in the literature concerning the use of montmorillonite clays from Burkina Faso for Pb^{2+} removal from water.

Heavy metal contamination of water represents a serious environmental and public health issue due to its accumulation in the food chain and its persistence in ecosystems [7]. The consumption of water contaminated with lead (Pb^{2+}) can cause numerous adverse health effects, including damage to the skin, respiratory system, lungs, cardiovascular system, kidneys, and nervous system, and may also induce certain types of cancer [8] [9]. In response to these risks, the World Health Organization (WHO) recommends a maximum allowable lead concentration of 0.01 mg/L in drinking water [8].

In Burkina Faso, this issue is particularly critical in rural areas of the Sahelian regions, where water scarcity is increasing and access to safe drinking water remains a major concern [2]. In light of water pollution resulting from anthropogenic activities and the growing scarcity of water resources, it is essential to develop effective strategies for the remediation of contaminated water. The development of accessible, low-cost, and locally available solutions represents a promising approach. Therefore, the objective of this study is to evaluate the efficiency of a

natural clay, abundant in Burkina Faso, for the removal of lead from raw water.

2. Materials and Experimental Methods

2.1. Materials

2.1.1. Raw Material Extraction Site

The raw material used in this study was collected in the village of Kombissiri, located approximately 45 km south of the city of Ouagadougou (Figure 1). The geographical coordinates of the sampling site are X: 0670355 and Y: 1334702. From a geological perspective (Figure 2), the site is situated on a clayey plateau that constitutes the highest topographic relief within the internal tonalite domain.

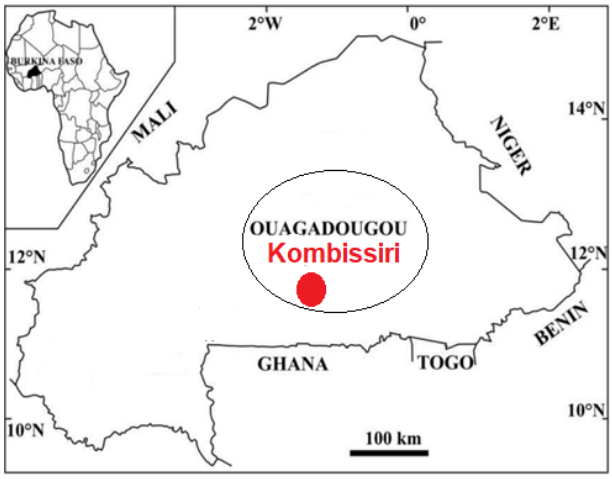

Figure 1. Location of study areas on the map of Burkina Faso.

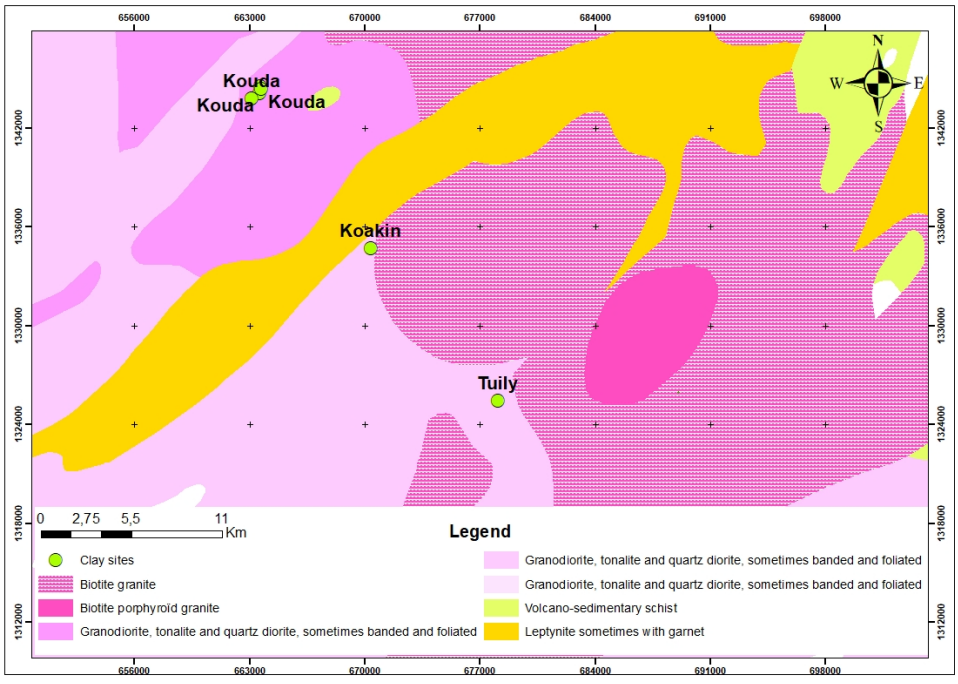

Figure 2. Geological map of Kombissiri.

2.1.2. Products

All solutions used in this work were prepared with ultrapure water with a resistivity of 18.2 MΩ·cm. The equipment used to prepare the various solutions was soaked in a bath of nitric acid (5%) for at least 12 hours and rinsed with ultrapure water before use. The Pb^{2+} solutions were prepared from lead nitrate $Pb(NO_2)_2$.

2.2. Experimental Methods

2.2.1. Characterization of Clay

Before undertaking the Pb^{2+} lead adsorption tests, KOM clay was fully characterised using various physicochemical techniques. Brunauer-Emmett-Teller (BET) analysis and Barrett-Joyner-Halenda (BJH) isotherm analysis (Micromeritics ASAP 2020 accelerated specific surface area and porosimetry system, Norcross, GA, USA) were used to determine the specific surface area, pore volume, and pore size of KOM clay, respectively.

Elemental chemical analysis was carried out using inductively coupled plasma atomic emission spectroscopy (ICP-AES, IRIS Intrepid II XSP). For this purpose, 0.25 g of clay sample was digested in a microwave digestion system using a mixture of 4 mL of HF (30% w/w), 3 mL of H_2SO_4 (96% w/w), and 3 mL of HNO_3 (65% w/w).

The mineralogical composition of the powdered sample was determined by X-ray diffraction (XRD) using a Siemens D5000 diffractometer equipped with a rear graphite monochromator. The instrument was operated at an accelerating voltage of 40 kV and a current of 30 mA, using a cobalt anode emitting Kα radiation with a wavelength of λ = 1.54 Å. Data acquisition and processing were controlled by DIFFRAC AT software (version 2).

Fourier transform infrared (FTIR) spectroscopy was performed using KBr pellets containing 2 wt.% of clay powder. Infrared spectra were recorded in the 400 - 4000 cm^{-1} range at a spectral resolution of 4 cm^{-1} using a Shimadzu FTIR-8400S spectrometer.

The morphology of the KOM clay powders was examined by scanning electron microscopy (SEM) using a HITACHI SU8020 microscope. Observations were carried out at an accelerating voltage of 30 kV, with magnifications up to 30,000X.

2.2.2. Semi-Quantification

Semi-quantitative analysis of the different mineral phases is performed by combining the results of X-ray diffraction and chemical analysis. This combination allows the relative quantities of minerals contained in KOM clay to be evaluated using Equation (1) [10]:

$$T(a) = \sum Mi \times Pi(a) \quad (1)$$

T(*a*): oxide content "*a*" in the sample, Mi: mineral content (%) "*i*" in the sample, *Pi*(*a*): proportion of oxide "*a*" in the mineral "*i*" (this proportion is deduced from the ideal formula attributed to the mineral "*i*").

2.2.3. Experimental Studies on Lead Removal

1) Adsorption kinetics

The adsorption kinetics were conducted to determine the equilibrium time between the adsorbent and the adsorbate. This is the time required for a thermodynamic equilibrium between the adsorbent and the adsorbate to be established [11]. The quantity Q_t of lead Pb^{2+} adsorbed by the clay as a function of time is calculated according to Equation (2):

$$Q_t = \left(V \times \left(C_0 - C_t\right)\right) / m \tag{2}$$

C_0 and C_t (mg/L) are the concentrations of lead Pb^{2+} at times t_0 and t, respectively.

V(L) and m (mg) are the volume of the solution and the dry mass of the clay used, respectively.

To evaluate the adsorption process of lead Pb^{2+} on KOM clay, the results of the effect of stirring time on adsorption were used to study two types of kinetic models (pseudo-first order and pseudo-second order). These models are represented by Equations (3) and (4), which are linear forms.

Pseudo-first-order model [11] [12].

$$\ln\left(\boldsymbol{Q}_e - \boldsymbol{Q}_t\right) = \ln\left(\boldsymbol{Q}_e\right) - \boldsymbol{k}_1 \times \boldsymbol{t} \tag{3}$$

Pseudo-second-order model [11] [12].

$$\boldsymbol{t}/\boldsymbol{Q}_t = 1/\left(\boldsymbol{K}_2 \times \boldsymbol{Q}_e^2\right) + \boldsymbol{t}/\boldsymbol{Q}_e \tag{4}$$

where $\boldsymbol{Q_t}$ is the amount of lead adsorbed at time t (mg/g), $\boldsymbol{k_1}$ is the pseudo-first-order kinetic constant in min^{-1}, $\boldsymbol{k_2}$ is the pseudo-second-order kinetic constant in g/mg·min, and $\boldsymbol{Q_e}$ is the amount of lead adsorbed at equilibrium in mg/g.

The graphical representation of $\ln\left(\boldsymbol{Q}_e - \boldsymbol{Q}_t\right)$ as a function of $\boldsymbol{t}$ allows the parameters of the pseudo-first-order model ($\boldsymbol{Q}_{e\_exp}$ and $\boldsymbol{k}_1$) to be determined.

The graph of $\left(\boldsymbol{t}/\boldsymbol{Q}_t\right)$ as a function of **t** allows us to determine $\boldsymbol{Q}_{e\_exp}$ and $\boldsymbol{k}_2$ respectively of the pseudo-second-order model.

2) Dose effect

A series of experiments were conducted by adapting the protocols proposed by Ennajih, H. [13]. Starting with stock solutions of lead Pb^{2+} (1000 mg/L), daughter solutions of lead with a concentration of 5 mg/L were prepared.

The method consists of placing 50 mL of a lead Pb^{2+} solution with a concentration of 50 mg/L in ten 250 mL polyethylene bottles. To this, we added increasing amounts of KOM clay, ranging from 0.1 to 1 g. All experiments were conducted according to the equilibrium time found during the adsorption kinetics.

The percentage of lead or the amount of lead is calculated using Equation (5).

$$\%\left(\boldsymbol{Pb}^{2+}\right) = \left(\left(\boldsymbol{C}_0 - \boldsymbol{C}_e\right)/\boldsymbol{C}_0\right) \times 100 \tag{5}$$

C_0 and C_e are the initial and final concentrations (mol/L) of lead in solution, respectively.

3) Effect of initial concentration

The effect of the initial concentration on the adsorption process was obtained by varying the initial concentration of lead (Pb^{2+}) from 5 to 80 mg/L, while maintaining the adsorbent dose at 0.5 g. Adsorption experiments were performed by contacting 0.5 g of clay with 50 mL of lead (Pb^{2+}) solutions with initial concentrations ranging from 5 to 80 mg/L in 250 mL polyethylene flasks at room temperature. The mixture was shaken for three hours. The solvent used to prepare the lead solutions is pure water with a resistivity of 18.2 MΩ·cm. After three hours of agitation, the solutions are collected and centrifuged at 3000 rpm for 15 minutes using a BECKMAN J2-MI centrifuge. Then, they are filtered using nylon membranes with a 0.45 µm retention threshold.

The amount (q_e) of lead fixed by a gram of adsorbent is given by Equation (6) [14].

$$Q_e = (C_0 - C_e) \times V/m \tag{6}$$

With:

m: Mass of the adsorbent (g).

Q_e : Quantity of lead per unit mass of adsorbent (mg/g).

C_0 : Initial lead concentration (mg/L).

C_e : Residual concentration of lead in the liquid phase at equilibrium (mg/L).

V: Volume of the adsorbate (L).

4) Isotherms of adsorption

To estimate the maximum adsorption capacity of the KOM clay and understand the lead (Pb^{2+}) adsorption mechanism by the KOM clay, an adsorption isotherm study was conducted.

The Langmuir model assumes that the adsorption process occurs via a monolayer on the adsorbent, that all the retention sites are homogeneous, that the number of retention sites is constant, and that adsorption occurs without interference. The Langmuir isotherm equation is given by Equation (7) [6].

$$C_e/Q_e = 1/Q_0K_L + C_e/Q_e \tag{7}$$

By plotting $C_e/Q_e = f(C_e)$, a straight line is obtained, $y = cx + d$, with a slope of $c = 1/Q_0$ and an ordinate at the origin of $d = 1/(Q_0K_L)$. K_L and Q_0 can be deduced by combining $K_L = C/d$ and $Q_0 = 1/C$.

In addition, the Langmuir isotherm can be expressed as a separation factor (R_L), which is given by equation 8 and indicates the nature of the adsorption process [14].

$$R_L = 1/((1 + K_L \cdot C_0)) \tag{8}$$

With C_0 as the initial concentration of the adsorbate in mg/L and K as the Langmuir constant.

The Freundlich isotherm is a special case of the Langmuir model where adsorption corresponds to heterogeneous multicomponent adsorption. Among other things, this model describes non-ideal physical adsorption.

The Freundlich model is described by Equation (9) [6].

$$\ln(Q_e) = \ln(K_F) + 1/n \ln(C_e) \quad (8)$$

By representing $\ln(Q_e) = f(\ln(C_e))$, we can deduce $1/n$ from the slope and K_F from the y-intercept. The heterogeneity condition is verified if $1 < n < 10$ [14].

K_F is the adsorption capacity in mg/g, C_e is the equilibrium concentration of the adsorbate, and $1/n$ is a constant indicating the intensity of adsorption.

3. Results and Discussion

3.1. Characterization of Clay

3.1.1. Physicochemical Characteristics

Knowledge of physicochemical characteristics is necessary to understand many adsorption phenomena [15]. The characterization results revealed that KOM clay has a specific surface area and porosity suitable for the adsorption of Pb^{2+}. The specific surface area of KOM clay, determined by the BET method, is 185.713 m^2/g. This value is significantly higher than the values reported in the literature for local montmorillonite clay for the adsorption of Pb^{2+} lead [16] [17].

It should also be noted that montmorillonite clay has relatively small average pore diameters (2.433 nm), almost at the limit of microporosity, as well as a large pore volume (0.101 cm^3/g) [17]. Figure 3 shows the pore size distribution curves for KOM clay.

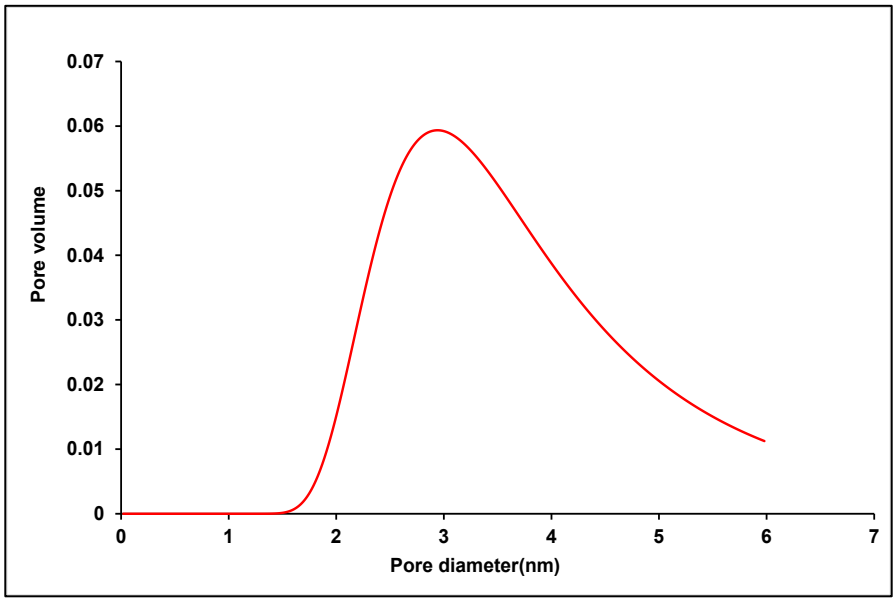

Figure 3. Pore size distribution curves of montmorillonite clay.

3.1.2. Chemical Analysis

Table 1 presents the results of the elemental chemical analysis of KOM. Analysis of these data shows that silica and alumina are the major oxides in the KOM sample, with iron, potassium, calcium, and magnesium oxides present in small quantities.

This composition is consistent with the chemical compositions of montmorillonite clays, which have been the subject of numerous studies on the removal of inorganic pollutants [2] [17] [18].

Table 1. Chemical composition of KOM clay in mass percent.

Oxides	SiO_2	Fe_2O_3	Al_2O_3	K_2O	CaO	MgO	MnO_2, BaO, NaO	PF	Total
%	49.22	5.69	18.40	2.47	1.07	2.35	<1.00	17.60 ± 1.50	100.06

3.1.2. X-Ray Diffraction Analysis

Figure 4 shows the X-ray diffractogram of the KOM sample. Examination of the diffractogram (Figure 4) reveals that the KOM sample is composed of quartz (SiO_2), montmorillonite ($(Na,Ca)_{0.3}(Al,Mg)_2Si_4O_{10}(OH)_2{\cdot}nH_2O$), Illite ($(K_{0.7}Al_2(Al_{0.7}Si_{3.3})O_{10}(OH)_2$), kaolinite ($Al_2Si_2O_5(OH)_4$), and goethite (FeO(OH)).

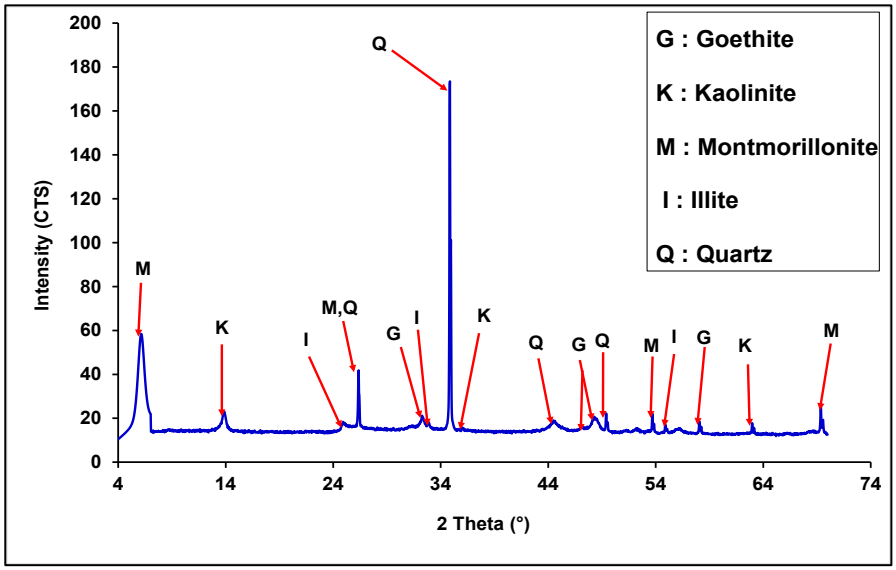

Figure 4. Diffractogram of montmorillonite clay KOM.

3.1.3. Infrared Analysis of the KOM Sample

Figure 5 shows the infrared spectrum of the KOM sample. The characteristic bands of the functional groups in the infrared spectrum were assigned based on the infrared tables provided in the literature (Table 2). The infrared spectrum shows three spectral regions. The first group is noted between 3650 and 3400 cm^{-1}, a second between 1650 and 900 cm^{-1}, and a third around 800 to 550 cm^{-1}.

3.1.4. Semi-Quantification

The semi-quantitative analysis of the different mineral phases present in the KOM sample was determined using XRD coupled with IR, and the data were recorded in Table 3. These results show that the KOM sample is composed of Quartz (SiO_2) (27%); Montmorillonite($(Na,Ca)_{0.3}(Al,Mg)_2Si_4O_{10}(OH)_2{\cdot}nH_2O$) (25%); Illite ($K_{0.7}Al_2(Al_{0.7}Si_{3.3})O_{10}(OH)_2$) (21%); kaolinite ($Al_2Si_2O_5(OH)_4$) (18%), and goethite (FeO(OH)) (6%).

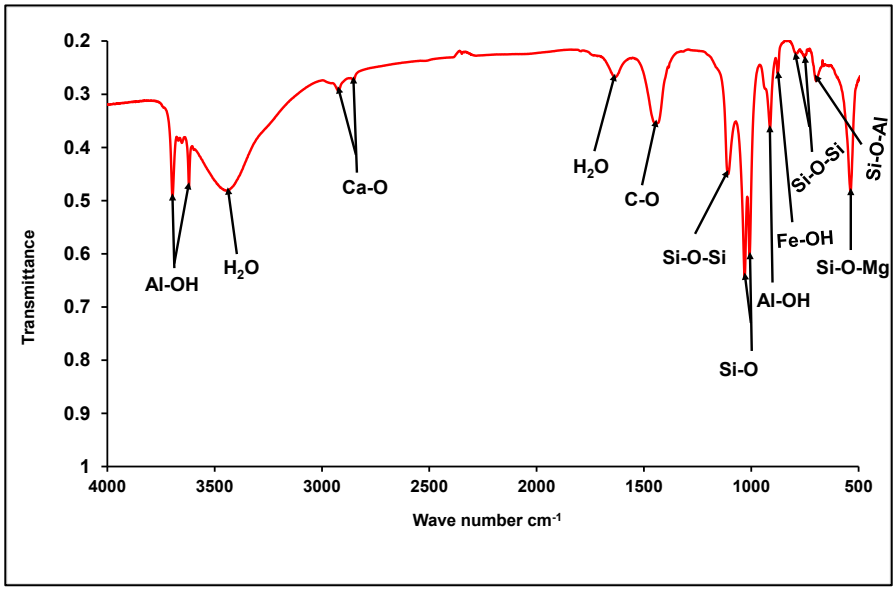

Figure 5. Infrared spectrum of the KOM sample.

Table 2. Interpretation of infrared spectra of KOM clay.

(en·cm^{-1})	Probable attributions	References
3697 et 3625	Bands attributable respectively to the external Al-OH bonds of kaolinite and the internal Al-OH bonds located between the Si_2O_5 tetrahedral layer and the $Al_2(OH)_6$ octahedral layer.	[19]
3439	Band corresponding to surface water molecules located in the interlayer (surface OH groups linked by hydrogen bonds).	[20]
2928 et 2851	Bands attributable respectively to the Ca-O bonds of montmorillonite	[21]
1103, 1028 et 1007	Bands attributable to silicates.	[20]
913	Bands attributable to silicates	[22]
873	Band attributable to the vibration of the Fe-OH bond in goethite.	[23]
790, 751 et 693	Si-O-Si and Si-O-Al vibration bands of kaolinite.	[24]
793	Bands attributable respectively to the Ca-O bonds of montmorillonite	[21]
793	Bands attributable respectively to the Si-O-Mg bonds of montmorillonite	[17] [24]

Table 3. Mineralogical composition of KOM montmorillonite clay in mass percent.

Mineral phase	Quartz	Montmorillonite	Illite	Kaolinite	Goethite	Total
% mass	27 ± 1	25 ± 1	21 ± 1	18 ± 1	6 ± 1	97

3.1.5. Morphology of the KOM Sample

The morphology of KOM clay was investigated by scanning electron microscopy (SEM), and the corresponding micrographs are presented in Figure 6. The SEM images reveal the presence of large, compact agglomerates composed of stacked pseudo-hexagonal platelets. These platelets exhibit a random spatial orientation and are consistently observed across all samples. Such microstructural features indicate a poorly ordered kaolinite phase within the clay matrix. Previous studies have demonstrated that iron-rich kaolinites commonly exhibit structural disorder

[22], which is consistent with the detection of iron oxide phases in KOM clay. Moreover, the pronounced cohesiveness observed in the KOM sample suggests the formation of micrometric agglomerates constituted of individual lamellar particles whose dimensions exceed those typically associated with kaolinite. This morphological characteristic further corroborates the presence of montmorillonite as a dominant or significant phase in the KOM clay [21].

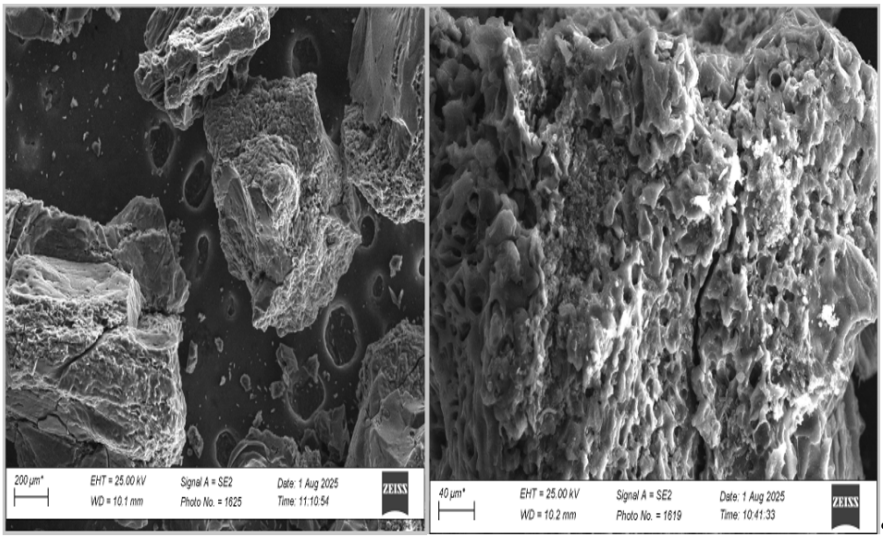

Figure 6. SEM image of montmorillonite clay KOM.

3.2. Lead Removal Using KOM Clay

3.2.1. Effect of Contact Time and Adsorption Kinetics

Figure 7 illustrates the amount of lead adsorbed per gram of KOM clay as a function of contact time. The results show a rapid increase in Pb^{2+} uptake during the first three hours, followed by a plateau beyond this period, indicating that adsorption equilibrium is reached after approximately 3 h. At equilibrium, the adsorption capacity (Q_t) is about 0.5 $mg{\cdot}g^{-1}$, corresponding to a removal efficiency exceeding 90% for an initial Pb^{2+} concentration of 50 $mg{\cdot}L^{-1}$. **Figure 8** further indicates that the equilibrium contact time remains unchanged for both KOM dosages (0.25 g and 0.5 g), suggesting that the adsorbent dose does not significantly influence the time required to reach equilibrium.

The kinetic data were analyzed using two commonly applied models: the pseudo-first-order kinetic model (**Figure 8(a)**) and the pseudo-second-order kinetic model (**Figure 8(b)**). Among these, the pseudo-second-order model provides the best fit to the experimental data, as evidenced by the higher coefficients of determination (R^2 = 0.996 and 0.998). Moreover, the experimentally determined equilibrium adsorption capacities (Q_e, exp) are in good agreement with the calculated values (Q_e, cal) obtained from the pseudo-second-order model (**Table 4**). These results indicate that Pb^{2+} adsorption onto KOM clay follows pseudo-second-order kinetics, suggesting that chemisorption mechanisms, such as inner-sphere complexation, play a dominant role in the adsorption process [12] [25].

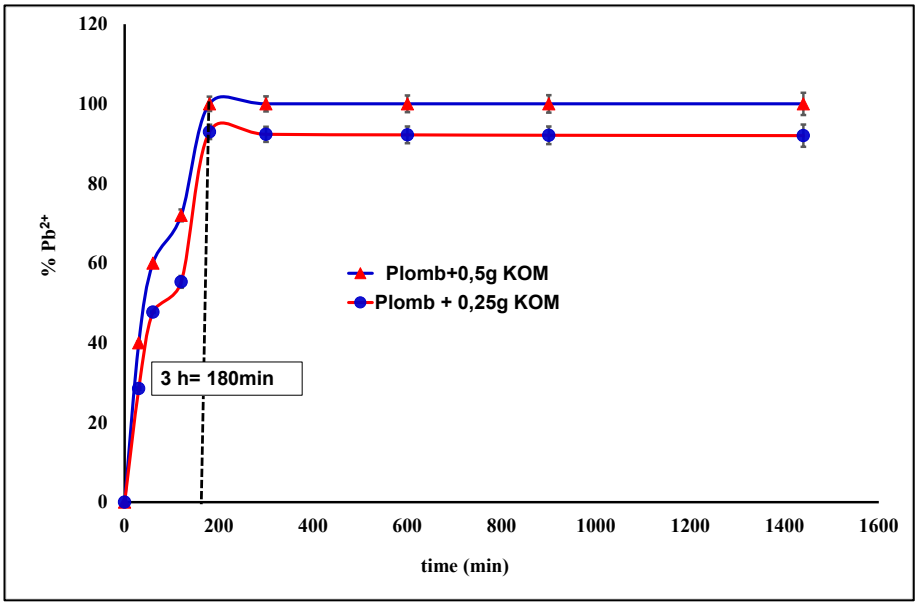

Figure 7. Effect of contact time.

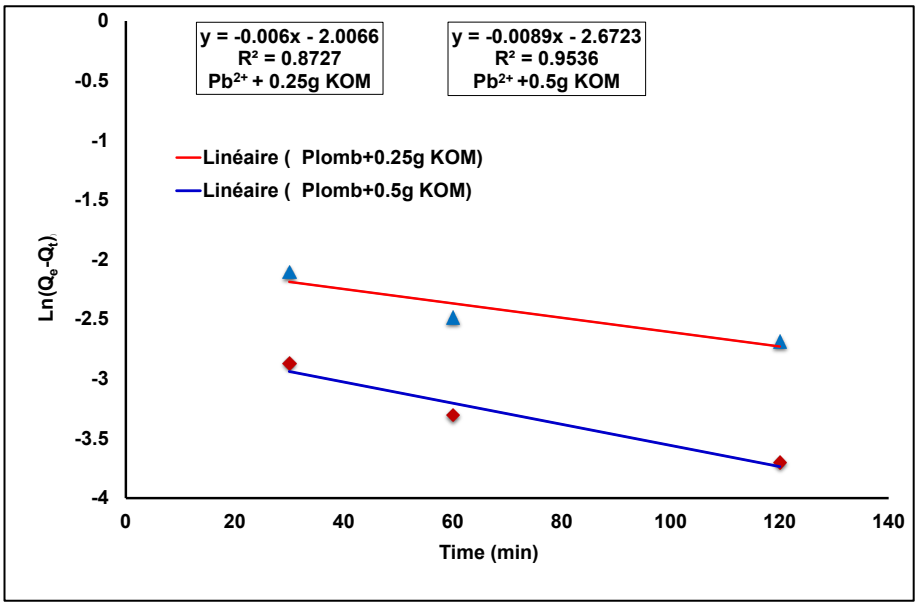

Figure 8. Kinetic models of Pb^{2+} lead adsorption. (a): pseudo-first-order kinetics and (b): pseudo-second-order kinetics.

Table 4. Kinetic parameters and correlation coefficients for lead adsorption on KOM clay.

Kinetic parameters and coefficients of determination								
	Pseudo-first-order model				Pseudo-second-order model			
Mass in g	Qe, exp (mg/g)	Qe, cal (mg/g)	k_1 (mn^{-1})	R^2	Qe, exp (mg/g)	Qe, cal (mg/g)	k_2 ($g{\cdot}mg^{-1}{\cdot}mn^{-1}$)	R^2
KOM (0.25 g)	0.178	0.134	0.006	0.866	0.178	0.190	0.134	0.996
KOM (0.5 g)	0.096	0.069	0.008	0.953	0.096	0.100	0.407	0.998

3.2.2. Dose Effect

The adsorbent dosage is a key parameter that significantly influences heavy metal removal from aqueous solutions, as it governs the adsorbent–adsorbate equilibrium of the system under investigation [26] [27]. **Figure 9** illustrates the effect of KOM clay dosage on Pb^{2+} removal. As the adsorbent dose increased from 0.1 to 1 g, the adsorption capacity decreased from 1.097 to 0.300 $mg{\cdot}g^{-1}$, while the Pb^{2+} removal efficiency increased from 54.88% to 97.30%.

The observed increase in removal efficiency with increasing adsorbent dosage can be attributed to the greater availability of active sorption sites on the clay surface [22] [28]. The higher number of adsorption sites resulting from the increased amount of adsorbent enhances Pb^{2+} uptake from solution, despite the concomitant decrease in adsorption capacity per unit mass, which is commonly associated with partial site saturation and possible particle aggregation at higher dosages [29] [30].

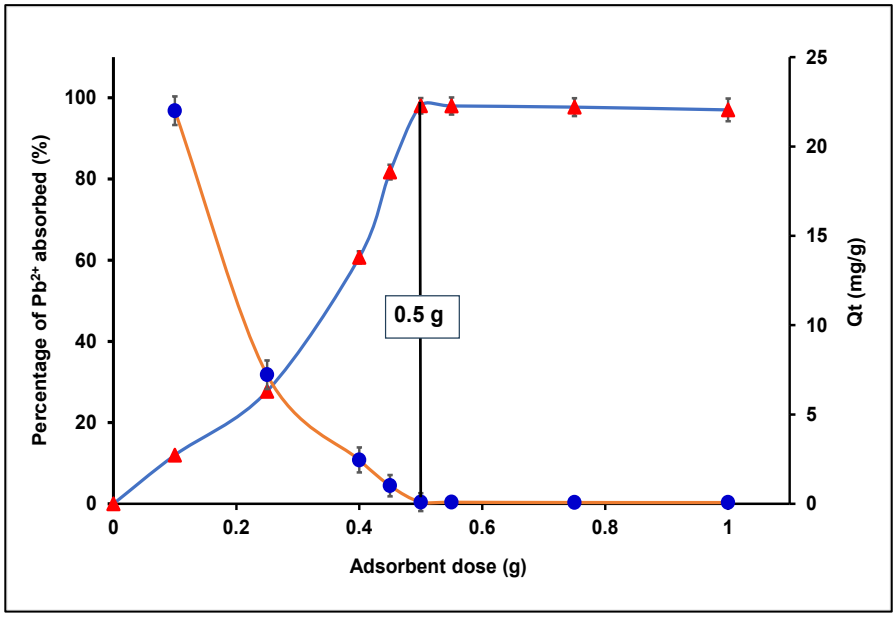

Figure 9. Effect of KOM montmorillonite clay dosage on Pb^{2+} adsorption rate = 50 mg/L; Adsorbent dosage = 0.1 - 1 g; Stirring time = 3 hours.

3.2.3. Effect of Initial Concentration

Figure 10 shows the effect of the initial concentration on the elimination of Pb^{2+}. This figure shows that the amount of Pb^{2+} adsorbed increases with the initial concentration of Pb^{2+}. This increase is due to a decrease in the solute's adsorption resistance as the concentration of Pb^{2+} increases [6].

3.2.4. Isotherms of Adsorption

The results of the initial concentration effect allowed us to model the adsorption isotherms (Langmuir and Freundlich). **Figure 11(a)** shows the Langmuir isotherm, **Figure 11(b)** shows the Freundlich isotherm, and the parameters of these adsorption isotherms are recorded in **Table 5**. An analysis of **Figure 11(a)** and

Figure 11(b) shows that the Langmuir model (R^2 = 0.9917) for the adsorption of Pb^{2+} by KOM clay is superior to the Freundlich model (R^2 = 0.9724). Consequently, the Langmuir isotherm best fits the experimental data. This suggests monolayer adsorption [6] [14].

In the present study, the RL values are between 0 and 1. This indicates that a monolayer adsorption process is favorable. These results are also confirmed by the R^2 determination coefficient. Combined with the Langmuir isotherm, the equilibrium RL values indicate that the clay used has good potential for adsorbing lead (Pb^{2+}) in an aqueous solution.

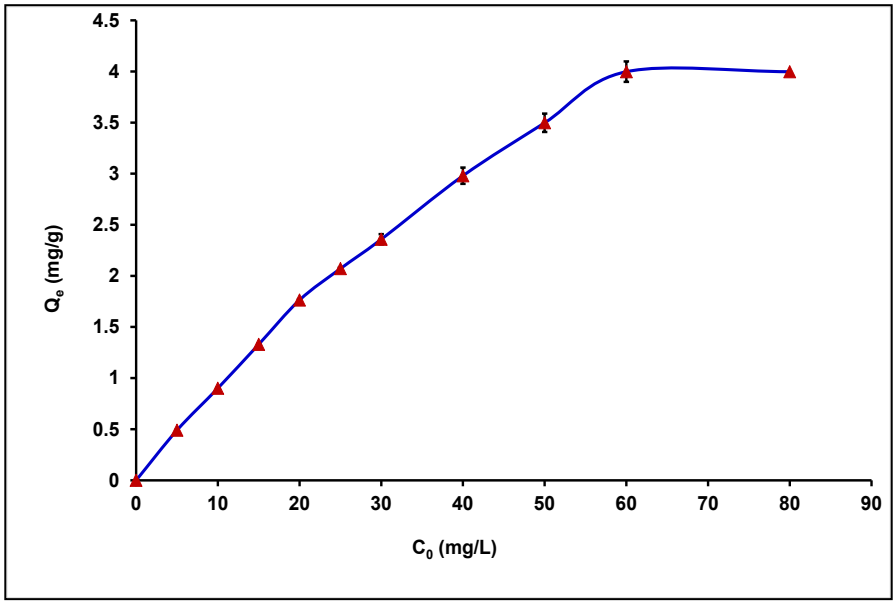

Figure 10. Effect of initial concentration on the adsorption rate of Pb^{2+}.

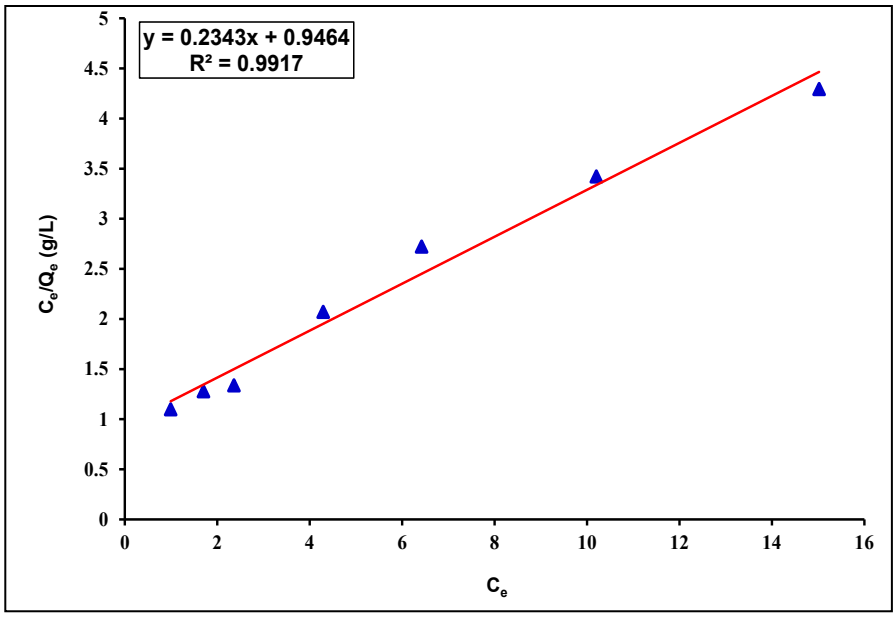

(a)

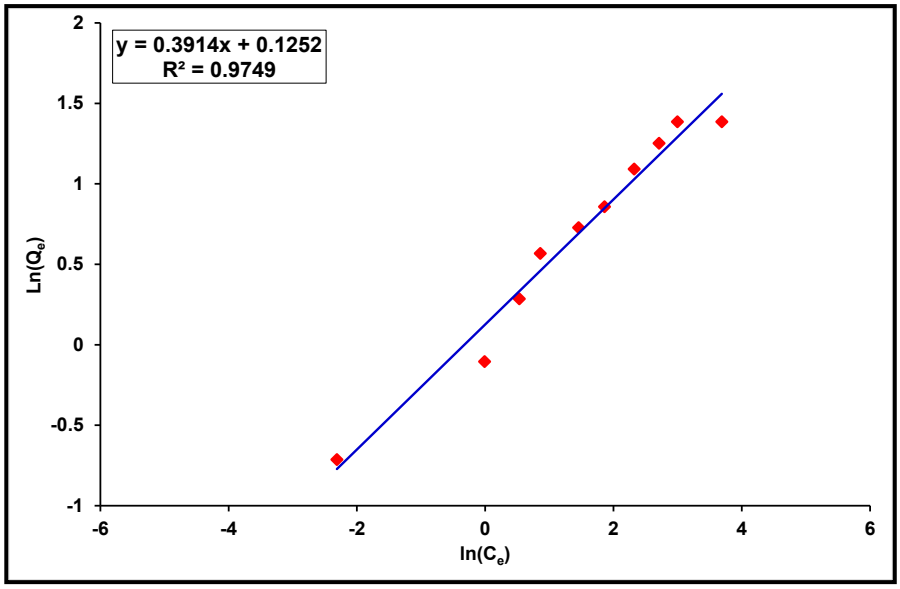

(b)

Figure 11. Modeling of Pb^{2+} adsorption isotherms. (a) Langmuir model; (b) Freundlich model.

Table 5. Parameters of the isotherms and determination coefficients.

	Langmuir model			Freundlich model		
R_L	KL (L/mg)	q_m (mg/g)	R^2	K_F (L/g)	n	R^2
0.4469	0.2475	4.268	0.9917	0.3403	2.5549	0.9749

4. Conclusions

This study provides a comprehensive characterization of KOM clay using a combination of analytical techniques, including BET surface area analysis, X-ray diffraction (XRD), infrared (IR) spectroscopy, chemical analysis, and scanning electron microscopy (SEM). This multidisciplinary approach yielded robust scientific data on the physicochemical properties of the clay. Mineralogical analysis based on XRD coupled with IR spectroscopy revealed that the KOM sample is composed primarily of quartz (SiO_2, 27%), montmorillonite ($(Na,Ca)_{0.3}(Al,Mg)_2Si_4O_{10}(OH)_2{\cdot}nH_2O$, 25%), illite ($K_{0.7}Al_2(Al_{0.7}Si_{3.3})O_{10}(OH)_2$, 21%), kaolinite ($Al_2Si_2O_5(OH)_4$, 18%), and goethite (FeO(OH), 6%).

BET analysis indicated that KOM clay exhibits a high specific surface area of 185.713 $m^2{\cdot}g^{-1}$ and a significant pore volume of 0.101 $m^3{\cdot}g^{-1}$, characteristics that are favorable for adsorption processes. The results obtained from chemical analysis and XRD were qualitatively confirmed by infrared spectroscopy, which identified the characteristic vibrational frequencies of functional groups associated with the different mineral phases present in the sample. The combined chemical and mineralogical features strongly suggest that KOM clay is a suitable adsorbent for Pb^{2+} removal from aqueous media.

Batch adsorption experiments demonstrated the effective removal of Pb^{2+} ions using KOM clay. A high removal efficiency of approximately 98%, corresponding to an adsorption capacity of 4.9 $mg \cdot g^{-1}$, was achieved at an adsorbent dosage of 10 $g \cdot L^{-1}$. Kinetic studies revealed that the adsorption process is relatively slow and follows a pseudo-second-order kinetic model, indicating that chemisorption, likely involving inner-sphere complexation mechanisms, governs Pb^{2+} uptake. The isotherm models obtained from the data on the effect of the initial concentration on the adsorption of lead Pb^{2+} confirmed that the adsorption of lead Pb^{2+} is monolayer adsorption. Combining the values of the equilibrium parameter RL with those of the Langmuir isotherm indicates that the clay used has good potential for adsorbing lead (Pb^{2+}) in aqueous solution.

Overall, KOM montmorillonite clay exhibits strong potential as a low-cost and efficient adsorbent for removing Pb^{2+} from groundwater.

Acknowledgments

The authors thank the ONEA (National Office for Water and Sanitation) for financial support.

Conflicts of Interest

The authors declare no conflict of interest.

References

[1] Kieufack, G., Fagel, N., Tchamba, A.B., Bomeni, I.Y., Ngapgue, F., El Ouahabi, M., *et al.* (2023) Mineralogical and Physico-Chemical Characterization of Alluvial Clays from Bamendou-Balessing (West Cameroon): Suitability for Ceramics. *Construction and Building Materials*, **407**, Article ID: 133396. https://doi.org/10.1016/j.conbuildmat.2023.133396

[2] Sorgho, B., Paré, S., Guel, B., Zerbo, L., Traoré, K. and Persson, I. (2011) Etude d'une argile locale du Burkina Faso à des fins de décontamination en Cu^{2+}, Pb^{2+} et Cr^{3+}. *Journal de la Société Ouest-Africaine de Chimie*, **31**, 49-59.

[3] Ukhurebor, K.E., Aigbe, U.O., Onyancha, R.B., Nwankwo, W., Osibote, O.A., Paumo, H.K., *et al.* (2021) Effect of Hexavalent Chromium on the Environment and Removal Techniques: A Review. *Journal of Environmental Management*, **280**, Article ID: 111809. https://doi.org/10.1016/j.jenvman.2020.111809

[4] Qlihaa, A., Dhimni, S., Melrhaka, F., Hajjaji, N. and Srhiri, A. (2016) Caractérisation physico-chimique d'une argile Marocaine [Physico-Chemical Characterization of a Morrocan Clay]. *Journal of Materials and Environmental Science*, **7**, 1741-1750. https://www.jmaterenvironsci.com/Document/vol7/vol7_N5/192-JMES-2132-Qlihaa.pdf

[5] Mekbel, S., Messaouda, D. and Ammar, N. (2024) Effets de l'argile et des boues sur le retrait et la porosité des briques : Etude comparative. International Society for Soil Mechanics and Geotechnical Engineering (ISSMGE). https://www.issmge.org/publications/online-library

[6] Mimanne, G., Benhabib, K., Benghalem, A. and Taleb, S. (2014) Etude de l'Adsorption des Métaux Lourds (Pb et Cd) en Solution Aqueuse sur Charbon Actif et Mont-

morillonite Sodée de l'Ouest Algérien [Study of the Adsorption of Heavy Metals (Pb and Cd) in Aqueous Solution on Activated Carbon and Sodium Montmorillonite from Western Algeria]. *Journal of Materials and Environmental Science*, **5**, 1298-1307. https://www.jmaterenvironsci.com/Document/vol5/vol5_N4/159-JMES-888-2014-Mimanne.pdf

[7] Imbga, B.K., Sorgho, B., Kabore, B. and Sambou, V. (2023) Caractéristiques thermiques d'une argile Kaolinite stabilisée avec la gousse de Néré en vue de l'isolation thermique de l'enveloppe du bâtiment dans la zone sahélienne. *Journal de Physique de la SOAPHYS*, **3**, C23N55-1-C23N55-7. https://doi.org/10.46411/jpsoaphys.2023.018

[8] Kouadio, L.M., Lebouachera, S.E.I., Blanc, S., Sei, J., Miqueu, C., Pannier, F., *et al.* (2022) Characterization of Clay Materials from Ivory Coast for Their Use as Adsorbents for Wastewater Treatment. *Journal of Minerals and Materials Characterization and Engineering*, **10**, 319-337. https://doi.org/10.4236/jmmce.2022.104023

[9] Generalova, A., Davidova, S. and Satchanska, G. (2025) The Mechanisms of Lead Toxicity in Living Organisms. *Journal of Xenobiotics*, **15**, Article 146. https://doi.org/10.3390/jox15050146

[10] Njopwouo, D. and Orliac, M. (1979) Note sur le comportement de certains minéraux A l'attaque triacide. In: *Cahiers de l ORSTOM, série Pédologie*, XVII, ORSTOM, 329-337.

[11] Ouedraogo, R.D., Bakouan, C., Sorgho, B., Guel, B. and Bonou, L.D. (2020) Caractérisation d'une latérite naturelle du Burkina Faso en vue de l'élimination de l'arsenic (III) et l'arsenic (V) dans les eaux souterraines. *International Journal of Biological and Chemical Sciences*, **13**, 2959-2977. https://doi.org/10.4314/ijbcs.v13i6.41

[12] Saeed, M., Munir, M., Nafees, M., Shah, S.S.A., Ullah, H. and Waseem, A. (2020) Synthesis, Characterization and Applications of Silylation Based Grafted Bentonites for the Removal of Sudan Dyes: Isothermal, Kinetic and Thermodynamic Studies. *Microporous and Mesoporous Materials*, **291**, Article ID: 109697. https://doi.org/10.1016/j.micromeso.2019.109697

[13] Taha, A.A., Shreadah, M.A., Ahmed, A.M. and Heiba, H.F. (2016) Multi-Component Adsorption of Pb(II), Cd(II), and Ni(II) onto Egyptian Na-Activated Bentonite; Equilibrium, Kinetics, Thermodynamics, and Application for Seawater Desalination. *Journal of Environmental Chemical Engineering*, **4**, 1166-1180. https://doi.org/10.1016/j.jece.2016.01.025

[14] Fayoud, N., Younssi, S.A., Tahiri, S. and Albizane, A. (2015) Etude cinétique et thermodynamique de l'adsorption de bleu de méthylène sur les cendres de bois. *Journal of Materials and Environmental Science*, **6**, 3295-3306.

[15] Ennajih, H. (2014) Synthèse de nouveaux surfactants pour la modification des argiles, étude et caractérisation des nanocomposites et biocomposites produits. Thèse de doctorat, Université Mohammed V, Agdal. https://toubkal.imist.ma/handle/123456789/13068

[16] Pleșa Chicinaș, R., Bedelean, H., Stefan, R. and Măicăneanu, A. (2018) Ability of a Montmorillonitic Clay to Interact with Cationic and Anionic Dyes in Aqueous Solutions. *Journal of Molecular Structure*, **1154**, 187-195. https://doi.org/10.1016/j.molstruc.2017.10.038

[17] Taha, A.A., Shreadah, M.A., Heiba, H.F. and Ahmed, A.M. (2017) Validity of Egyptian Na-montmorillonite for Adsorption of Pb^{2+}, Cd^{2+} and Ni^{2+} under Acidic Conditions: Characterization, Isotherm, Kinetics, Thermodynamics and Application Study. *Asia-Pacific Journal of Chemical Engineering*, **12**, 292-306. https://doi.org/10.1002/apj.2072

[18] Cai, J., Lei, M., Zhang, Q., He, J., Chen, T., Liu, S., *et al.* (2017) Electrospun Composite Nanofiber Mats of Cellulose@Organically Modified Montmorillonite for Heavy Metal Ion Removal: Design, Characterization, Evaluation of Absorption Performance. *Composites Part A*: *Applied Science and Manufacturing*, **92**, 10-16. https://doi.org/10.1016/j.compositesa.2016.10.034

[19] Garcia-Valles, M., Alfonso, P., Martínez, S. and Roca, N. (2020) Mineralogical and Thermal Characterization of Kaolinitic Clays from Terra Alta (Catalonia, Spain). *Minerals*, **10**, Article 142. https://doi.org/10.3390/min10020142

[20] Muwawa, J., Seke Vangu, M., Kayembe Sungula, J., Sola, D., Nkodi Mananga, T., Pongo Pongo, H., *et al.* (2024) Physicochemical Characterization by AXRF and XRD Analysis of Clays Samples from Bulungu, Kwilu Province, Democratic Republic of Congo. *Journal Africain des Sciences*, **1**, 64-69. https://doi.org/10.70237/jafrisci.2024.v1.i2.08

[21] Costa, T.C.d.C., Melo, J.D.D. and Paskocimas, C.A. (2013) Thermal and Chemical Treatments of Montmorillonite Clay. *Ceramics International*, **39**, 5063-5067. https://doi.org/10.1016/j.ceramint.2012.11.105

[22] Kouadio, L. M. (2023) Contribution à l'évaluation des niveaux de contamination des eaux et des sols des sites d'orpaillage clandestin et élimination des métaux (Hg, Pb, Cd) et de l'arsenic des eaux polluées, à l'aide des argiles de Côte d'Ivoire. Thèse de Doctorat, Université Felix Houphouët-Boigny, 1-232. https://hal.science/tel-04148757

[23] Sorgho, B., Bressollier, P., Guel, B., Zerbo, L., Ouedraogo, R., Gomina, M., *et al.* (2016) Étude des propriétés mécaniques des géomateriaux argileux associant la décoction de Parkia Biglobosa (néré). *Comptes Rendus. Chimie*, **19**, 895-901. https://doi.org/10.1016/j.crci.2016.01.016

[24] Munvuyi, D., Ousmane, M.S. and Bougouma, M. (2022) Physicochemical and Mineralogical Characterization of Clays from the Tcheriba Zone in the Boucle of Mouhoun Region (Burkina Faso). *Journal of Materials and Environmental Science*, **13**, 755-767. http://www.jmaterenvironsci.com

[25] Messeaouda, S. (2015) Etude de la capacité de rétention et d'élimination des cations métalliques par des adsorbants naturels. Thèse de Doctorat, Université de Mustapha Stambouli, 184 p. http://dspace.univ-mascara.dz:8080/jspui/handle/123456789/142.

[26] Ahmad, R. and Hasan, I. (2015) L-Cystein Modified Bentonite-Cellulose Nanocomposite (Cellu/Cys-Bent) for Adsorption of Cu^{2+}, Pb^{2+}, and Cd^{2+} Ions from Aqueous Solution. *Separation Science and Technology*, **51**, 381-394. https://doi.org/10.1080/01496395.2015.1095211

[27] Lacaran, J.V.T., Narceda, R.J., Bilo, J.A.V. and Leaño Jr., J.L. (2021) Citric Acid Crosslinked Nanofibrillated Cellulose from Banana (Musa Acuminata X Balbisiana) Pseudostem for Adsorption of Pb^{2+} and Cu^{2+} in Aqueous Solutions. *Cellulose Chemistry and Technology*, **55**, 403-415. https://doi.org/10.35812/cellulosechemtechnol.2021.55.38

[28] Gallouze, H., Akretche, D., Daniel, C., Coelhoso, I. and Crespo, J.G. (2021) Removal of Synthetic Estrogen from Water by Adsorption on Modified Bentonites. *Environmental Engineering Science*, **38**, 4-14. https://doi.org/10.1089/ees.2020.0048

[29] Kedi, A.B.B., Kouassi, S.S., Coulibaly, V. and Sei, J. (2021) Elimination de polluants des déchets liquides d'une unité de production de sucre par des argiles naturelles de Côte d'Ivoire. *International Journal of Biological and Chemical Sciences*, **15**, 803-815. https://doi.org/10.4314/ijbcs.v15i2.31

[30] Amor, G., & Bagane, M. (2021) Optimisation de l'adsorption du plomb et du zinc en solution bicomposé sur une argile activée par la méthode des plans d'expériences. I*OSR Journal of Engineering*, **11**, 2250-3021.